

# Hydration dynamics of aqueous glucose probed with polarization-resolved fs-IR spectroscopy

C.C.M. Groot<sup>1, a)</sup> and H.J. Bakker<sup>1</sup>

*FOM Institute AMOLF, Ultrafast spectroscopy group, Science Park 104, 1098 XG Amsterdam,  
The Netherlands*

(Dated: 22 July 2014)

The dynamics of water in aqueous solutions of glucose have been investigated using polarization-resolved femtosecond infrared spectroscopy of the hydroxyl stretch vibrations of water and glucose. Using reference measurements on solutions of glucose in DMSO and a spectral decomposition model, we are able to distinguish the reorientation dynamics of the glucose and water hydroxyl groups. We find that the water reorientation dynamics strongly slow down in the presence of glucose.

PACS numbers: 78.47.jb, 82.30.Rs

## I. INTRODUCTION

Sugars and water are extremely important in biology, and many studies have been devoted to their role in living systems. Sugars for example serve as energy source in most organisms and (when part of a glycoprotein or glycolipid) as signalling groups. Nevertheless, several biological processes involving sugars and water are not well understood. An example is the so-called bioprotective effect, which is the ability of sugars to stabilize proteins in the native folded state under extremely cold and dry conditions<sup>1</sup>. This effect is used by living organisms in extreme environments and widely applied in industry and biochemistry labs. One explanation for the bioprotective effect of sugars is that the interaction between sugars and water leads to a modification of the water structure and dynamics, which in turn affects the conformation of dissolved proteins<sup>2-6</sup>.

Sugars interact quite favorably with water molecules, as a sugar molecule contains multiple hydrophilic hydroxyl groups that can form stable hydrogen bonds with water molecules. In the past decades, the interaction between sugars and water has been studied with several experimental techniques. With THz absorption measurements an increase in absorption coefficient is observed relative to bulk water, which suggests a change of the hydrogen-bond network around the sugar<sup>2,3</sup>. From the deviation of linear ideal-mixing absorption changes, and the assumption that this deviation arises from the overlap of the hydration shells, the glucose hydration shell radius is estimated to be 3-4 Å. For disaccharides this radius is found to increase to 5-8 Å. Neutron scattering<sup>5,6</sup>, neutron diffraction<sup>7</sup> and Raman spectroscopy experiments<sup>5,8,9</sup> all provided evidence that the hydrogen bond network of water surrounding sugars differs from the structure of bulk water, but the difference is quite small<sup>7,8</sup>.

The dynamical effects of sugars on water are observed to be substantially stronger. The water translational and

reorientational dynamics around saccharides are slowed down significantly compared to bulk water, as shown by dynamic light scattering<sup>10,11</sup>, dielectric relaxation<sup>12</sup> and NMR<sup>13</sup> experiments, as well as MD simulations<sup>9</sup>. In most papers this effect is explained by the formation of strong hydrogen bonds between sugar and water. Molecular dynamics simulations show that the sugar-bonded water has a longer hydrogen bond lifetime<sup>14</sup> and is spatially constrained. Since the water reorientation rate depends on the rate of hydrogen bond breaking and the availability of a new hydrogen bond partner<sup>15</sup>, the water mobility is reduced<sup>2,3,9</sup>. The precise amount of retardation and its spatial extent are still under debate. In dynamic light scattering experiments a relaxation process is observed that is about 5-6 times slower than the orientational relaxation of bulk water, and that is assigned to hydration water<sup>10</sup>. The spectral amplitude of this process indicates that in the dilute limit approximately 3.3 water molecules are slowed down per sugar hydroxyl, but the exact amplitude is difficult to determine because it is masked by the sugar rotational relaxation. Recent NMR experiments report a retardation of the water <sup>17</sup>O relaxation rate<sup>13</sup>. Assuming only the first hydration layer is affected, a modest dynamic retardation factor of 1.67 is found. Unfortunately, with NMR experiments it is not possible to determine the hydration shell size and dynamic retardation factor independently. So in effect, while it is clear that sugars in water induce a slowing down of water dynamics, the magnitude of the effect remains to be determined.

Here we report on a study of the dynamics of water in aqueous solutions of glucose using polarization-resolved femtosecond infrared spectroscopy. This technique allows a direct measurement of the reorientation dynamics of individual water and glucose hydroxyl groups on a sub-picosecond timescale. The measurements provide molecular-scale insight into the dynamics of the hydration shell of glucose.

---

<sup>a)</sup> Electronic mail: cgroot@amolf.nl

## II. EXPERIMENT

We measure the vibrational and reorientation dynamics of water and glucose using polarization-resolved femtosecond infrared spectroscopy. Aqueous glucose solutions are prepared by adding glucose (purity >99.5%), from Sigma-Aldrich) to ultrapure water (Milli-Q grade) at concentrations ranging from 1 to 10 molal (moles per kg solvent). To optimize the dissolution the solutions are stirred and heated to 50 °C. After cooling back to room temperature the glucose stays well-dissolved. In addition, 4% of the water and glucose hydroxyl groups are deuterated by adding a small amount of heavy water ( $D_2O$ ). The deuterated hydroxyl (OD) groups have a strong absorption at  $2500\text{ cm}^{-1}$ , associated with the OD stretch vibration. We excite and probe this vibration to measure the picosecond orientational dynamics of the OD group.

The infrared excitation and probe pulses are generated by frequency conversion of the output of a Ti:sapphire based regenerative amplifier. This amplifier produces  $800\text{ }\mu\text{J}$  pulses centered at 800 nm at a repetition rate of 1 kHz. Part of the light is used to pump a BBO-based optical parametric amplifier. The resulting  $2\text{ }\mu\text{m}$  idler beam is subsequently frequency doubled in a second BBO crystal and mixed with the remaining 800 nm light in a lithium niobate crystal. This difference frequency generation process produces  $7\text{ }\mu\text{J}$  pulses at  $2500\text{ cm}^{-1}$  with  $100\text{ cm}^{-1}$  bandwidth and 200 fs pulse duration. In most experiments part of the pulse is split off by a wedged plate to use as a probe pulse. In another experiment an independently tunable probe pulse is generated by a separate optical parametric amplifier. The probe pulses are dispersed in a grating-based spectrometer and detected with a 3x32 pixel mercury-cadmium-telluride (MCT) detector array.

The excitation with the main part of the  $7\text{ }\mu\text{J}$ , 200 fs infrared pulse leads to transient absorption changes that are monitored by the probe pulse. These absorption changes contain two contributions. Firstly, the excitation leads to a decreased absorption around  $2500\text{ cm}^{-1}$  due to bleaching of the ground-state absorption and stimulated emission out of the vibrationally excited state. Secondly, there is an increased absorption around  $2300\text{ cm}^{-1}$  associated with the absorption from the first excited state of the vibration to the second excited state. By changing the pump-probe delay we measure the time dependence of the signals, which provides information on the lifetime of the vibration. Since we use broadband excitation pulses that cover the whole OD stretch absorption band, the effects of spectral diffusion are negligible. In addition to the vibrational signal associated with the excitation of the  $v=1$  state of the OD stretch vibration, there is a smaller signal due to sample heating. As the energy of the excited vibration is ultimately transferred into heat, this signal grows in with delay.

We probe the transient absorption at the fundamental  $v=0\rightarrow 1$  transition around  $2500\text{ cm}^{-1}$ . Probing this transition has advantages over probing the  $1\rightarrow 2$  transition:

the smaller spectral width of the  $v=0\rightarrow 1$  transition leads to stronger signals and allows us to probe the complete transient spectral response of the glucose and water OD oscillators. In addition, the  $v=1\rightarrow 2$  transition overlaps with the strong absorption of  $CO_2$  in air, which means that this band can only be accurately measured in case the setup would be purged with nitrogen.

We measure the transient spectral response with probe pulses polarized parallel and perpendicular to the polarization direction of the pump. Since the pump primarily excites OD vibrations aligned to the pump polarization, the transient absorption signal measured with the parallel polarized probe pulse will initially be larger than the signal measured with the perpendicular polarized probe pulse. At longer delay times the signals will become equal due to the randomization of the orientation of the excited OD oscillators.

From the parallel ( $\Delta\alpha_{||}$ ) and perpendicular ( $\Delta\alpha_{\perp}$ ) probe signals we construct the isotropic signal<sup>16</sup>,

$$\Delta\alpha_{iso}(\nu, t) = \frac{1}{3}(\Delta\alpha_{||}(\nu, t) + 2\Delta\alpha_{\perp}(\nu, t)) \quad (1)$$

where  $\nu$  signifies the probe frequency and  $t$  the pump-probe delay. The isotropic signal decays with the lifetime of the OD stretch vibration and is independent of molecular reorientation. The normalized difference between the parallel and perpendicular probe signals corresponds to the anisotropic signal<sup>16</sup>,

$$R(\nu, t) = \frac{\Delta\alpha_{||}(\nu, t) - \Delta\alpha_{\perp}(\nu, t)}{\Delta\alpha_{||}(\nu, t) + 2\Delta\alpha_{\perp}(\nu, t)} \quad (2)$$

In the absence of Förster energy transfer between vibrations, the anisotropic signal decays with the molecular reorientation rate.  $R$  is proportional to the second-order rotational correlation function, which also contains librational contributions in the first 0.5 ps after the excitation. The time window for which we can accurately determine the anisotropy depends on the vibrational lifetime, since vibrational relaxation leads to a decrease of both the numerator and the denominator of Eq. (2).

To calculate the anisotropy signal associated with the vibrational excitation, the parallel and perpendicular absorption signals need to be corrected for the ingrowing heating signal mentioned earlier. The heating signal results from a rise in the sample equilibrium temperature after excitation and subsequent relaxation of OD oscillators. As such, its spectral signature is similar to the thermal difference spectrum, and only the amplitude of the heating signal changes with delay time. During the first few picoseconds after excitation, the local heating effect might lead to a slightly different spectral change than at later delay times. However, even if such a different thermal spectral response would be present at early delay times, its contribution to the total spectrum will be small as in the first few picoseconds the contribution of the thermal signal is small compared to the signal associated with the excitation of the OD stretch vibration. We determine the delay-time dependence of the heating signal by probing the transient absorption in the spectral

region between 2800 and 3000  $\text{cm}^{-1}$ , following excitation of the OD vibration at 2500  $\text{cm}^{-1}$ .<sup>17</sup> Between 2800 and 3000  $\text{cm}^{-1}$  the spectral changes associated with the excitation of the  $\nu=1$  state of the OD stretch vibration are negligibly small, and the absorption is dominated by the low frequency tail of the water OH stretch vibrations and the CH vibrations of glucose. As these vibrations are not directly excited by the 2500  $\text{cm}^{-1}$  pump pulse, their response only changes as a result of thermal effects following the relaxation of the OD stretch vibration. The dynamics of the response in this spectral region thus directly represents the dynamics of the heating. Combining the dynamics of the rise of the heating signal with its spectral response - which is the transient spectrum at long delays - we can accurately correct the parallel and perpendicular signals at all delay times and frequencies for the heating contribution.

### III. RESULTS

#### A. Isotropic and anisotropic signals

Figure 1a displays the isotropic vibrational signal for three different concentrations of aqueous glucose. These spectra are corrected for the ingrowing heat signal. The heat dynamics corresponding to the data of Figure 1 are shown in Figure 2c. With increasing concentration of glucose, the heat dynamics slow down. This can be explained by the fact that glucose is larger and heavier than water and as such will require more time to adapt its position to the higher local temperature. For all concentrations of glucose, the isotropic vibrational signal shows a transient absorption decrease (bleaching signal) around 2500  $\text{cm}^{-1}$  and the onset of an excited state absorption at lower frequencies. With increasing concentration of glucose, the vibrational relaxation becomes more inhomogeneous over the OD stretch absorption band, showing a faster decay on the red side and a slower decay on the blue side of this band. In Figure 1b we present the anisotropic signals corresponding to the isotropic signals of Figure 1a. With increasing concentration of glucose, the anisotropy decay becomes slower and increasingly frequency dependent.

In Figure 2a we show the isotropic signal measured at 2500  $\text{cm}^{-1}$  as a function of delay time for different concentrations of glucose. For water without any added glucose the signal decays with a relaxation time constant of  $\sim 1.7$  ps, which agrees with previous observations of the lifetime of the OD stretch vibration<sup>18</sup>. In Figure 2b we show the anisotropy dynamics corresponding to the isotropic signals of Figure 2a. For pure water the anisotropy decays with a time constant of 2.5 ps, in agreement with previous work on the molecular reorientation of bulk water<sup>18</sup>. As glucose is added, the anisotropy decay slows down dramatically.

#### B. Disentangling contributions from water and glucose - spectral decomposition model

The signals shown in Figures 1 and 2 contain contributions from both water and glucose OD stretch vibrations. These contributions need to be disentangled in order to study the effect of glucose on the dynamics of water. To clarify the contribution of the glucose hydroxyl vibrations to the signals of Figures 1 and 2, we performed similar measurements on a solution of partly deuterated glucose in dimethylsulfoxide (DMSO). DMSO is a highly polar solvent like water, but unlike water does not contain hydroxyl vibrations. Hence, for this solution the signals measured in the frequency region of the OD stretch vibration only represent the hydroxyl vibrations of glucose. In Figure 3a we show transient spectra measured for a solution of 0.4 molal glucose in DMSO. We observe a bleaching signal around 2500  $\text{cm}^{-1}$  and the onset of an induced (excited-state) absorption at frequencies  $< 2420 \text{ cm}^{-1}$ . The decay of the bleaching is observed to be highly frequency-dependent, being much faster on the red side of the OD absorption band than on the blue side of this band. The transient spectra at all delay times can be modeled well with the two bands shown in Figure 3c. These bands decay mono-exponentially with time constants of  $1.4 \pm 0.1$  ps and  $4.6 \pm 0.1$  ps. The associated anisotropy decays of the two bands are shown in Figure 3d. It is seen that these anisotropy decays are quite slow in comparison to the anisotropy decay of bulk water. For the low-frequency band, the decay of the anisotropy is negligible in the time range of  $\sim 10$  ps of the experiment.

Based on this knowledge, we analyze the data for the glucose in water solutions shown in Figures 1 and 2 with a spectral decomposition model in which we define one vibrational band for water and two vibrational bands for glucose. In this model, we fix the spectral shape and vibrational relaxation of the water band to the corresponding parameters of bulk HDO:H<sub>2</sub>O, and we assume that the spectral shapes, vibrational relaxation rates, and anisotropy decays of the two glucose bands do not change with the concentration of glucose. The amplitudes of the glucose bands relative to the water band are determined by the concentration of glucose. Each spectral band is assumed to have an associated frequency independent anisotropy, of the form

$$R_i(t) = A_i e^{-t/\tau_{ri}} + B_i \quad (3)$$

The only parameters that are allowed to vary with concentration are the parameters describing the anisotropy decay of the water band. We fit this model with few free parameters to all recorded isotropic and anisotropic signals in one single least-squares fit, by adding up square errors at each iteration step. The isotropic signal is spectrally decomposed in the three bands  $\sigma_i$  for a particular set of mono-exponentially decaying populations  $N_i$ . The error is then determined by comparing the isotropic signal at all delay times with the sum spectrum resulting

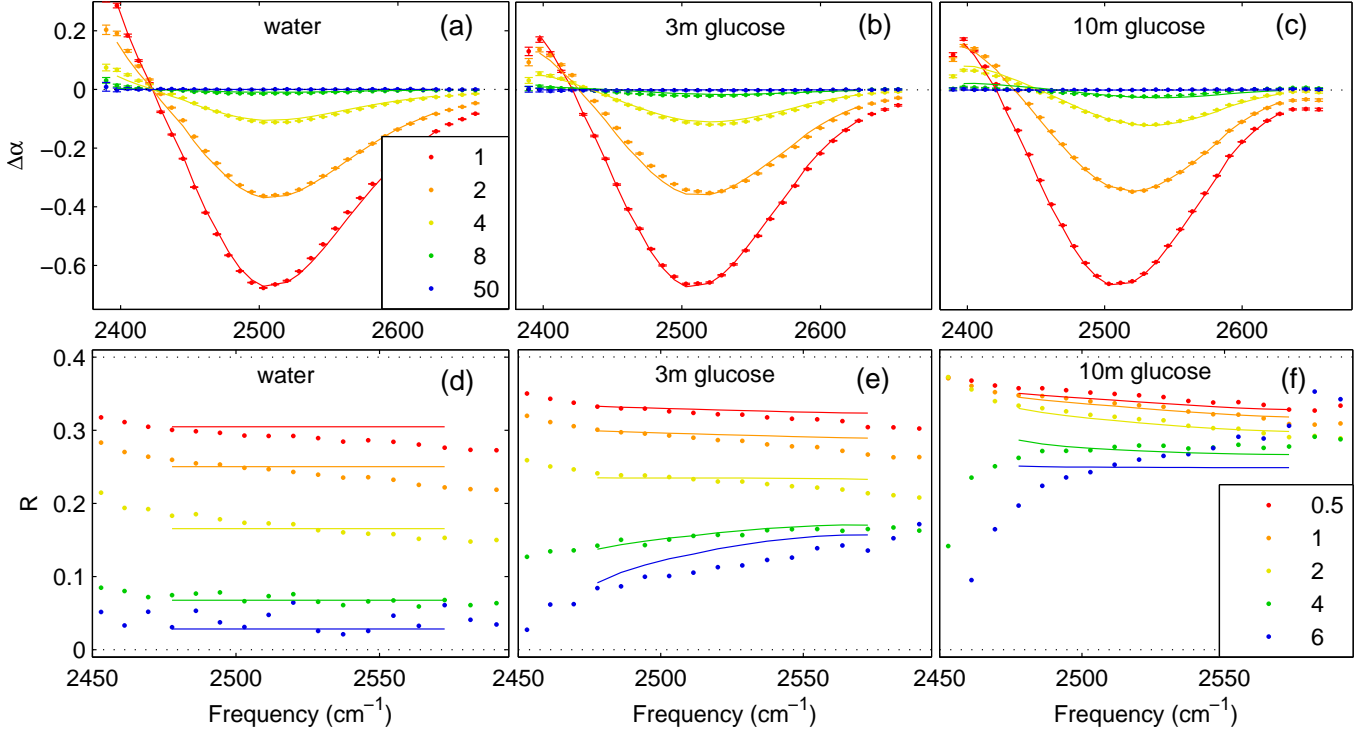


FIG. 1. The isotropic absorption change (upper panels) and the anisotropy of the absorption change (lower panels) as a function of frequency at five different delay times. The spectra are corrected for the heating contribution to the signal. Shown are the results for three different glucose concentrations. The lines are calculated with the model described in the text of the manuscript.

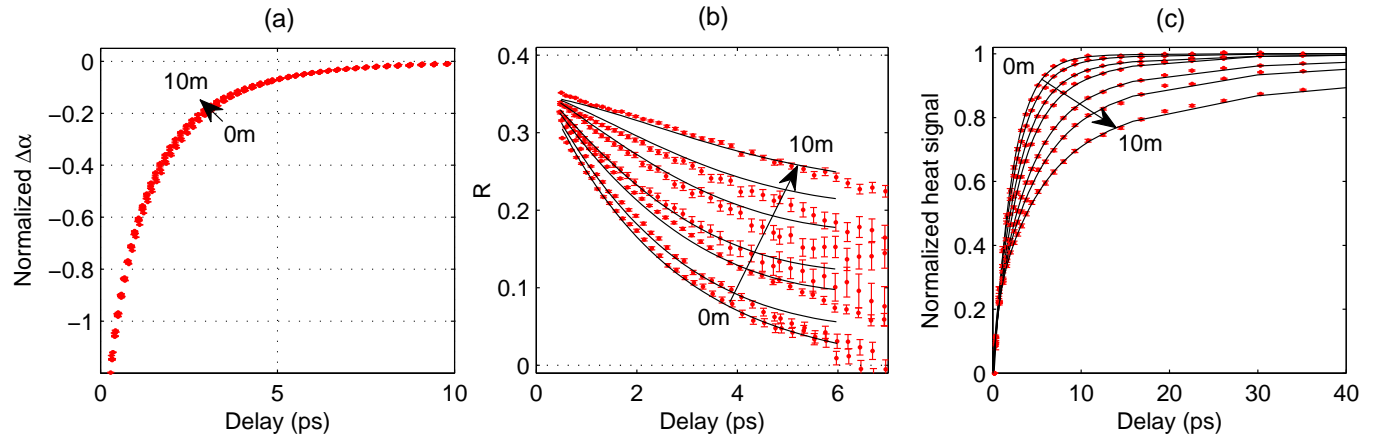


FIG. 2. (a): The isotropic absorption change at  $2500 \text{ cm}^{-1}$ , (b): the anisotropy of the absorption change at  $2500 \text{ cm}^{-1}$ , and (c): the normalized heat dynamics, as measured between  $2800-3000 \text{ cm}^{-1}$ , as a function of delay time for solutions of glucose in water of different concentration (0, 1, 2, 3, 5, 7 and 10 m). The solid lines in (b) are obtained with the model described in the text. The solid lines in (c) represent an empirical triple-exponential fit to the data.

from the three spectral components

$$\sum_i N_i(t) \sigma_i(\nu) \quad (4)$$

In addition each model anisotropy component  $R_j$  (given by model  $A_j, \tau_{rj}$  and  $B_j$ ) is compared to the following

quantity:

$$\frac{\frac{1}{3}(\alpha_{\parallel} - \alpha_{\perp}) - \sum_{i \neq j} R_i N_i \sigma_i}{N_j \sigma_j} \quad (5)$$

Here  $\alpha_{\parallel}$  and  $\alpha_{\perp}$  are the parallel and perpendicular ab-

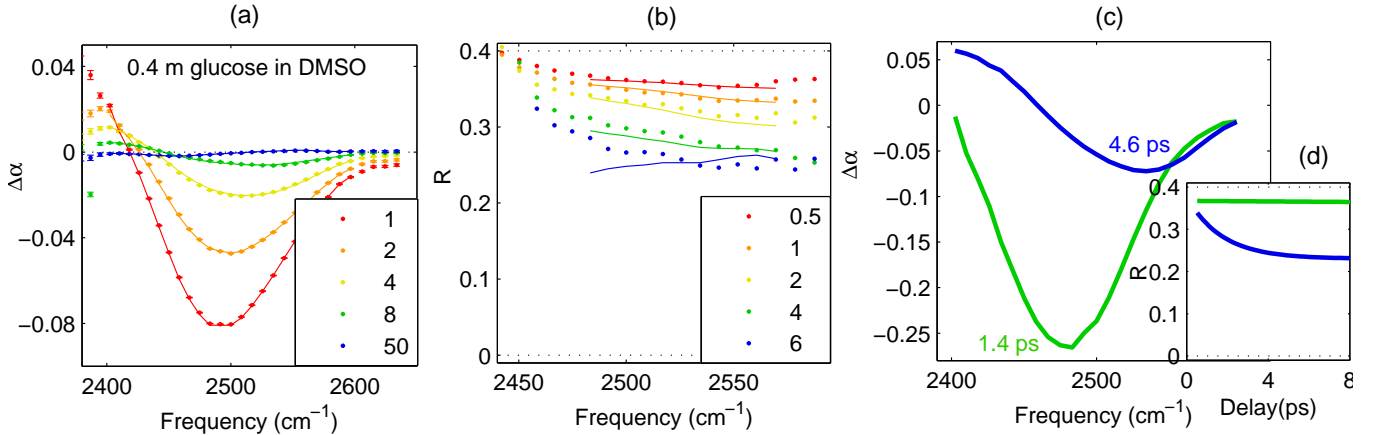


FIG. 3. (a): The isotropic absorption change and (b): the anisotropy of the absorption change, as a function of frequency for a solution of 0.4 m glucose (10% deuterated) in DMSO. (c): The spectral components resulting from a fit of the data with the spectral decomposition model described in the text, and (d): the anisotropy of the two spectral components as a function of delay time.

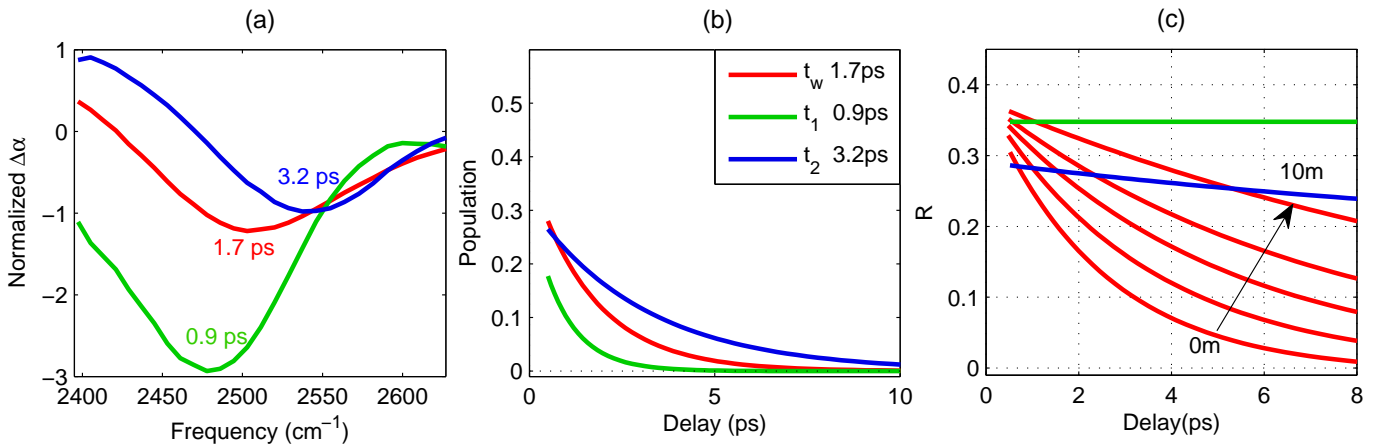


FIG. 4. (a): Spectral components of the isotropic absorption change measured for a solution of 10 molal glucose in water. (b): The population of the three spectral components as a function of delay time for the same solution. The solid lines are obtained directly from the spectral relaxation model, the points are obtained by decomposing the transient spectra at each delay time in the spectral components shown in (a). (c): The anisotropy of the two glucose components and the water component for solutions of 0, 3, 5, 7 and 10 molal glucose in water.

sorption signals. In Eq. (5) we make use of the fact that

$$\frac{1}{3}(\alpha_{\parallel} - \alpha_{\perp}) = \sum_i R_i N_i \sigma_i \quad (6)$$

For faster convergence the right and left side of Eq. (6) are compared in each iteration step as well.

We fit this model to all recorded data. The results of the fit are represented by the solid curves in Figures 1 and 2 and are found to be in good agreement with the data. The spectral band shapes resulting from the fit are illustrated in Figure 4a. The vibrational relaxation dynamics and anisotropy dynamics of these bands are shown in Figures 4b and 4c, respectively. The good agreement between our model and the data at all recorded delay times and frequencies, shows that our assumption that the three bands have the same spectral

shape and lifetime at all concentrations of glucose is justified. The spectral shapes of the glucose bands are very similar to the bands we observed before for the solutions of glucose in DMSO. The bands are shifted by 10-20  $\text{cm}^{-1}$  with respect to the water band and have a smaller width by about 15  $\text{cm}^{-1}$ . The shift leads to a broadening of the total transient spectra, but the narrowing mostly undoes this effect, which is why the transient spectra for different glucose concentrations have a similar shape, as shown in Figure 1. The lifetimes of the two glucose bands are  $0.9 \pm 0.2$  ps and  $3.2 \pm 0.2$  ps, shorter than in DMSO, which can be explained from the higher density of low-frequency intermolecular accepting modes in the water solvent. The anisotropy dynamics of the glucose bands is very similar to the dynamics observed in DMSO. Again, these dynamics are very slow in comparison to the anisotropy

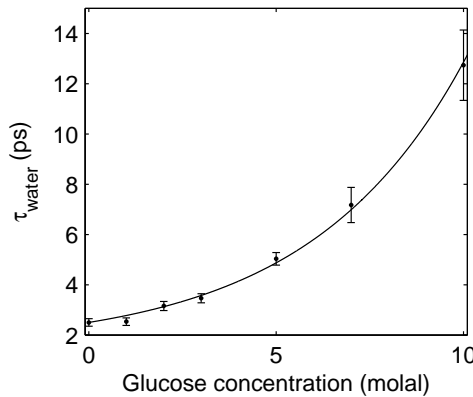


FIG. 5. Water reorientation time constant as a function of glucose concentration. Solid line is guide to the eye.

dynamics of bulk water. We find that the anisotropy decays very slowly with a relaxation time of 10-20 ps for the high-frequency band, and more than 20 ps for the low frequency band. The anisotropy decay of the water band is much faster, but slows down strongly with increasing concentration of glucose. We find that we can describe the water anisotropy at each glucose concentration without including a constant anisotropy end level, as the fit parameter B stays within  $\pm 0.01$  from zero for all concentrations. Hence, for all glucose concentrations the water anisotropy decay is described well with a single reorientation time constant.

In Figure 5 we present the reorientation time constant  $\tau_r$  of the water band as a function of concentration. The time constant strongly increases with concentration.

#### IV. DISCUSSION

##### A. Glucose dynamics

We have found that the transient spectral response of hydrogen-bonded glucose molecules can be well described with two spectral bands showing different vibrational relaxation times and different anisotropy dynamics. The two bands do not necessarily represent two distinct species of glucose hydroxyl groups. They can rather represent a continuous distribution of relaxation times across the glucose OD stretch band. The red side of the glucose OD stretch band corresponds to strongly hydrogen bonded hydroxyl groups, while the blue side corresponds to weakly hydrogen bonded hydroxyl groups. We find that strongly hydrogen bonded groups have a shorter vibrational lifetime, which is a quite generally observed trend<sup>19</sup>. The shorter lifetime can be explained by the increase of the anharmonic coupling to the low-frequency intermolecular accepting modes of the solvent hydrogen bond network.

The hydroxyl groups of glucose show little anisotropy

decay within the  $\sim 10$  ps time window of the experiment. For weakly hydrogen-bonded hydroxyl there is only a fractional decay of the anisotropy, and for strongly hydrogen-bonded hydroxyl groups the decay is even negligible. The absence of significant anisotropy decay for the glucose hydroxyl groups suggests that the donated hydrogen bond of the hydroxyl group remains intact for a long time. This finding agrees with the results of molecular dynamics simulations that show that water-glucose hydrogen bonds are very stable<sup>14</sup>. The lack of significant anisotropy decay also indicates that the complete solvation structure of the glucose molecule and its hydration shell barely reorient within the time scale of the experiment. This notion agrees with previous studies, in which it was found that glucose molecules in water reorient with an average time constant of  $\sim 33$  ps<sup>11</sup>. This rotational motion contributes only slightly to the anisotropy decay we observe. The limited anisotropy decay and its frequency dependence can be assigned to a wobbling motion of the hydroxyl group during which the hydrogen bond remains intact. The amplitude of this partial anisotropy decay is smaller at lower hydroxyl stretch vibrational frequencies, because for stronger hydrogen bonds the wobbling motion is constrained to a smaller cone angle.

##### B. Water dynamics

We found that the reorientation of water molecules slows down with increasing concentration of glucose. Interestingly, at all concentrations the water reorientation can be well described by a single exponential function. This finding indicates that the reorientation time constants of the water molecules in a solution of glucose form a single-peaked distribution. This observation stands in strong contrast with the results of earlier studies of the reorientation dynamics of water in solutions of small amphiphiles<sup>20</sup> and salts<sup>21,22</sup>. For these solutions we observed clear bi-exponential decays, indicative of a bimodal distribution of reorientation time constants. The slower time constant could be assigned to the reorientation dynamics in the hydration shell of the solute. For amphiphiles in solution, it was found that part of the water molecules reorient with the same time constant as in bulk water, while another part is strongly slowed down by a factor 4-5 compared to the bulk<sup>23,24</sup>. The slow water molecules are located in the hydration shells of the hydrophobic molecular groups of the amphiphiles<sup>23,24</sup>. In the experiments on salt solutions, often a slow component is observed as well; this component is associated with water molecules donating a hydrogen bond to the anion<sup>21,22</sup>. For glucose in water solutions we cannot make such a clear distinction between the dynamics of the hydration shell and the bulk. This indicates that for glucose in water, the transition from the hydration shell to the bulk is more diffuse than for ions or the hydrophobic groups of small amphiphilic molecules. The observation that the anisotropy dynamics can be modeled well with a single

slow average reorientation time at all glucose concentrations, indicates that the slowdown effect of glucose on water is not distinctively strong for water molecules near glucose and that the slowdown effect is quite long-range.

The effect of glucose on the reorientation dynamics of water will be primarily associated with the interactions between water and the hydrophilic hydroxyl groups of the glucose molecule. These hydrophilic groups will accept and donate hydrogen bonds to water molecules and thereby participate in the hydrogen-bonding network of water. In view of the strong directional character of hydrogen bonds, a donated bond from glucose to water influences the orientation of the hydrogen-bonded water, which in turn can affect the orientation of the surrounding water molecules. This view is consistent with experimental evidence that carbohydrates slightly modify the water structure<sup>5-9</sup>. A slight change in water structure could have a strong effect on the water dynamics. It has been shown that molecular reorientation in liquid water proceeds via water molecules in special hydrogen-bonded configuration, in which the hydroxyl groups forms a weak, bifurcated hydrogen bond to two other water molecules. Hence, a donated hydrogen bond from glucose to water can influence the dynamics over several water molecules. This interaction is fundamentally different from water molecules in the hydration shells of anions. For the latter system it has been observed that the hydroxyl group that donates a hydrogen bond to the anion - and is aligned towards it - shows different dynamics from the other hydroxyl groups. However, this effect cannot propagate to other water molecules, because an anion like  $\text{Cl}^-$  or  $\text{I}^-$  does not have an preferred binding direction, and the water molecules are still free to move over the anion surface. Our current hypothesis is consistent with the findings of molecular dynamics simulations<sup>14</sup> that show the formation of stable sugar-water hydrogen bonds, with a small structural modification of the water network and a strong slow down of water reorientation as a result.

The present results are consistent with the results of dielectric relaxation measurements of aqueous glucose solutions as well<sup>12</sup>. The dielectric relaxation (DR) spectra show a distribution of relaxation times that broadens with glucose concentration. The principal relaxation time, which is proportional to the first order rotational correlation function, strongly increases with glucose concentration. In fact, this time constant increases faster with concentration than the water reorientation time constant we measure (Figure 5). The viscosity of aqueous glucose, which is proportional to the molecular reorientation rate as well, increases even faster<sup>12</sup>. While fs-IR spectroscopy is sensitive to molecular-scale reorientation, DR spectroscopy measures a more collective dipolar reorientation response. So by going from fs-IR to DR to viscosity measurements, one effectively goes from a probe of dynamics at the molecular scale to a probe of dynamics at the macroscopic scale. The stronger increase of the dielectric relaxation time constant and viscosity with

glucose concentration can thus be explained from the fact that these parameters probe the collective reorientation and translation dynamics of water and glucose. In our experiment we selectively determine the dynamics of the water molecules, since we can distinguish the water and glucose hydroxyl contributions to the measured transient absorption spectra by their spectral signatures. The advantage of our technique is that such a distinction is possible.

Considering the bioprotective effect, our results show that sugars lead to a slowdown of the hydrogen-bond and molecular reorientation dynamics of water over relatively large length scales. It is conceivable that these changes in water dynamics in turn affect the conformational structure and dynamics of dissolved proteins.

## V. CONCLUSION

The dynamics of water in aqueous solutions of glucose have been investigated using polarization-resolved femtosecond infrared spectroscopy. With increasing concentration of glucose, the hydroxyl stretch vibrational relaxation becomes more inhomogeneous, showing a faster decay on the red side of the OD stretch band and a slower decay on the blue side of this band. We find that this inhomogeneity is caused by the response of the glucose hydroxyl stretch vibrations. The inhomogeneous relaxation of the glucose vibrations can be modeled with two spectral bands that decay with different time constants. The response of the water hydroxyl stretch vibrations can be modeled well with a single spectral band with a vibrational lifetime of  $\sim 1.7$  ps that remains the same at all glucose concentrations.

Thanks to the spectral decomposition, we can distinguish the anisotropy dynamics of the water and the glucose hydroxyl groups. This allows us to obtain information on the separate reorientation dynamics of these groups. We find that the glucose hydroxyl groups only show a restricted wobbling motion within the  $\sim 10$  ps time scale of the experiment. The cone angle of the wobbling motion is slightly larger on the blue side of the spectrum. The water hydroxyl groups show a much faster reorientation ( $\sim 2.5$  ps for water without any added glucose), but this reorientation slows down with increasing concentration of glucose. Interestingly, at all glucose concentrations the orientational dynamics of the water molecules can be well described with a single exponential function. Compared to the effect of ions and hydrophobic molecules on water dynamics, the effect of glucose is weaker but much longer ranged.

## ACKNOWLEDGMENTS

This work is part of the research program of the Stichting voor Fundamenteel Onderzoek der Materie (FOM), which is financially supported by the Nederlandse organ-

isatie voor Wetenschappelijk Onderzoek (NWO). The research is financially supported by NanoNextNL as well.

- <sup>1</sup>L. M. Crowe, R. Mouradian, J. H. Crowe, S. A. Jackson, and C. Womersley, *Biochimica et Biophysica Acta (BBA) - Biomembranes* **769**, 141 (1984).
- <sup>2</sup>U. Heugen, G. Schwaab, E. Bründermann, M. Heyden, X. Yu, D. M. Leitner, and M. Havenith, *Proceedings of the National Academy of Sciences* **103**, 12301 (2006).
- <sup>3</sup>M. Heyden, E. Bründermann, U. Heugen, G. Niehues, D. M. Leitner, and M. Havenith, *Journal of the American Chemical Society* **130**, 5773 (2008).
- <sup>4</sup>A. M. Massari, I. J. Finkelstein, B. L. McClain, A. Goj, X. Wen, K. L. Bren, R. F. Loring, and M. D. Fayer, *Journal of the American Chemical Society* **127**, 14279 (2005), pMID: 16218622.
- <sup>5</sup>C. Branca, S. Magazù, G. Maisano, S. M. Bennington, and B. Fák, *The Journal of Physical Chemistry B* **107**, 1444 (2003).
- <sup>6</sup>F. Affouard, P. Bordat, M. Descamps, A. Lerbret, S. Magazù, F. Migliardo, A. Ramirez-Cuesta, and M. Telling, *Chemical Physics* **317**, 258 (2005).
- <sup>7</sup>S. E. Pagnotta, S. E. McLain, A. K. Soper, F. Bruni, and M. A. Ricci, *The Journal of Physical Chemistry B* **114**, 4904 (2010).
- <sup>8</sup>M. E. Gallina, P. Sassi, M. Paolantoni, A. Morresi, and R. S. Cataliotti, *The Journal of Physical Chemistry B* **110**, 8856 (2006).
- <sup>9</sup>A. Lerbret, F. Affouard, P. Bordat, A. Hédoux, Y. Guinet, and M. Descamps, *Journal of Non-Crystalline Solids* **357**, 695 (2011).
- <sup>10</sup>L. Lupi, L. Comez, M. Paolantoni, S. Perticaroli, P. Sassi, A. Morresi, B. M. Ladanyi, and D. Fioretto, *The Journal of Physical Chemistry B* **116**, 14760 (2012).
- <sup>11</sup>D. Fioretto, L. Comez, M. Gallina, A. Morresi, L. Palmieri, M. Paolantoni, P. Sassi, and F. Scarponi, *Chemical Physics Letters* **441**, 232 (2007).
- <sup>12</sup>K. Fuchs and U. Kaatze, *The Journal of Chemical Physics* **116** (2002).
- <sup>13</sup>L. R. Winther, J. Qvist, and B. Halle, *The Journal of Physical Chemistry B* **116**, 9196 (2012).
- <sup>14</sup>S. L. Lee, P. G. Debenedetti, and J. R. Errington, *The Journal of Chemical Physics* **122**, 204511 (2005).
- <sup>15</sup>D. Laage and J. T. Hynes, *Science* **311**, 832 (2006).
- <sup>16</sup>G. Seifert, T. Patzlaff, and H. Graener, *Vibrational Spectroscopy* **23**, 219 (2000).
- <sup>17</sup>S. T. van der Post, *Love and fear of water : water dynamics around charged and apolar solutes*, Ph.D. thesis, University of Amsterdam (2014).
- <sup>18</sup>Y. L. A. Rezus and H. J. Bakker, *The Journal of Chemical Physics* **123**, 114502 (2005).
- <sup>19</sup>H. J. Bakker, *Chemical Reviews* **108**, 1456 (2008).
- <sup>20</sup>Y. L. A. Rezus and H. J. Bakker, *Phys. Rev. Lett.* **99**, 148301 (2007).
- <sup>21</sup>S. T. van der Post, S. Scheidelaar, and H. J. Bakker, *Journal of Molecular Liquids* **176**, 22 (2012).
- <sup>22</sup>S. T. van der Post, K.-J. Tielrooij, J. Hunger, E. H. G. Backus, and H. J. Bakker, *Faraday Discuss.* **160**, 171 (2013).
- <sup>23</sup>C. Petersen, K.-J. Tielrooij, and H. J. Bakker, *The Journal of Chemical Physics* **130**, 214511 (2009).
- <sup>24</sup>K.-J. Tielrooij, J. Hunger, R. Buchner, M. Bonn, and H. J. Bakker, *Journal of the American Chemical Society* **132**, 15671 (2010).